

Histopathological patterns in atypical teratoid/rhabdoid tumors are related to molecular subgroup



Francesca Zin, Jennifer A. Cotter, Christine Haberler, Matthias Dottermusch, Julia Neumann, Ulrich Schüller, Leonille Schweizer, Christian Thomas, Karolina Nemes, Pascal-David Johann, Marcel Kool, Michael C. Frühwald, Werner Paulus, Alexander Judkins, Martin Hasselblatt

Angaben zur Veröffentlichung / Publication details:

Zin, Francesca, Jennifer A. Cotter, Christine Haberler, Matthias Dottermusch, Julia Neumann, Ulrich Schüller, Leonille Schweizer, et al. 2021. "Histopathological patterns in atypical teratoid/rhabdoid tumors are related to molecular subgroup." *Brain Pathology* 31 (5): e12967. <https://doi.org/10.1111/bpa.12967>.

RESEARCH ARTICLE

Histopathological patterns in atypical teratoid/rhabdoid tumors are related to molecular subgroup

Francesca Zin¹ | Jennifer A. Cotter² | Christine Haberler³ | Matthias Dottermusch⁴ | Julia Neumann⁴ | Ulrich Schüller^{4,5,6}  | Leonille Schweizer⁷ | Christian Thomas¹ | Karolina Nemes⁸ | Pascal D. Johann^{8,9,10,11} | Marcel Kool^{9,10,12} | Michael C. Frühwald⁸ | Werner Paulus¹ | Alexander Judkins² | Martin Hasselblatt¹ 

¹Institute of Neuropathology, University Hospital Münster, Münster, Germany

²Department of Pathology and Laboratory Medicine, Children's Hospital Los Angeles, Keck School of Medicine, University of Southern California, Los Angeles, CA, USA

³Division of Neuropathology and Neurochemistry, Department of Neurology, Medical University of Vienna, Vienna, Austria

⁴Institute of Neuropathology, University Medical Center, Hamburg-Eppendorf, Hamburg, Germany

⁵Research Institute Children's Cancer Center Hamburg, Germany

⁶Department of Pediatric Hematology and Oncology, University Medical Center, Hamburg-Eppendorf, Hamburg, Germany

⁷Department of Neuropathology, Berlin Institute of Health, Charité-Universitätsmedizin Berlin, Corporate Member of Freie Universität Berlin, Humboldt-Universität Zu Berlin, Berlin, Germany

⁸Pediatric and Adolescent Medicine, Swabian Children's, Cancer Center, University Children's, Hospital Medical Center Augsburg and EU-RHAB Registry, Augsburg, Germany

⁹Hopp Children's Cancer Center (KiTZ), Heidelberg, Germany

¹⁰Division of Paediatric Neurooncology, German Cancer Research Center (DKFZ), German Cancer Consortium (DKTK, Heidelberg, Germany)

¹¹Department of Pediatric Hematology and Oncology, University Hospital Heidelberg, Heidelberg, Germany

¹²Princess Máxima Center for Pediatric Oncology, Utrecht, The Netherlands

Correspondence

Martin Hasselblatt, Institute of Neuropathology, University Hospital Münster, Pottkamp 2, Münster 48149, Germany.
Email: hasselblatt@uni-muenster.de

Funding information

DFG, Grant/Award Number: HA 3060/8-1; IZKF Münster, Grant/Award Number: Ha3/017/20. Open Access funding enabled and organized by Projekt DEAL. WOA Institution: N/A Blended DEAL : Projekt DEAL.

Abstract

Atypical teratoid/rhabdoid tumor (AT/RT) is a highly malignant tumor that may not only contain rhabdoid tumor cells but also poorly differentiated small-round-blue cells as well as areas with mesenchymal or epithelial differentiation. Little is known on factors associated with histopathological diversity. Recent studies demonstrated three molecular subgroups of AT/RT, namely ATRT-TYR, ATRT-SHH, and ATRT-MYC. We thus aimed to investigate if morphological patterns might be related to molecular subgroup status. Hematoxylin-eosin stained sections of 114 AT/RT with known molecular subgroup status were digitalized and independently categorized by nine blinded observers into four morphological categories, that is, "rhabdoid," "small-round-blue," "epithelial," and "mesenchymal." The series comprised 48 ATRT-SHH, 40 ATRT-TYR, and 26 ATRT-MYC tumors. Inter-observer agreement was moderate but significant (Fleiss' kappa = 0.47; 95% C.I. 0.41-0.53; $p < 0.001$) and there was a highly significant overall association between morphological categories and molecular subgroups for each of the nine observers ($p < 0.0001$). Specifically, the category

This is an open access article under the terms of the Creative Commons Attribution-NonCommercial-NoDerivs License, which permits use and distribution in any medium, provided the original work is properly cited, the use is non-commercial and no modifications or adaptations are made.

© 2021 The Authors. Brain Pathology published by John Wiley & Sons Ltd on behalf of International Society of Neuropathology.

“epithelial” was found to be over-represented in ATRT-TYR ($p < 0.000001$) and the category “small-round-blue” to be over-represented in ATRT-SHH ($p < 0.01$). The majority of ATRT-MYC was categorized as “mesenchymal” or “rhabdoid,” but this association was less compelling. The specificity of the category “epithelial” for ATRT-TYR was highest and accounted for 97% (range: 88–99%) whereas sensitivity was low [49% (range: 35%–63%)]. In line with these findings, cytokeratin-positivity was highly overrepresented in ATRT-TYR. In conclusion, morphological features of AT/RT might reflect molecular alterations and may also provide a first hint on molecular subgroup status, which will need to be confirmed by DNA methylation profiling.

KEYWORDS

AT/RT, cytokeratin, DNA methylation profiling, histopathology, INI-1

1 | INTRODUCTION

Atypical teratoid/rhabdoid tumor (AT/RT) is a highly malignant central nervous system tumor mainly occurring in infancy and childhood (1). The designation “teratoid/rhabdoid” coined by Lucy B. Rorke-Adams (2, 3) reflects the notion that AT/RT may not only contain rhabdoid cells similar to malignant rhabdoid tumors of the kidney but also poorly differentiated small round blue cells as well as areas of mesenchymal or epithelial differentiation. The variety of morphological patterns represented a diagnostic problem and some also argued that such heterogeneity could not be compatible with a distinct entity (4). The immunohistochemical staining profile of AT/RT is also diverse with frequent positivity for vimentin and epithelial membrane antigen, but a proportion of cases also expressing cytokeratin, actin, GFAP, and/or neuronal markers (3). However, it soon became obvious that bi-allelic mutations of SWI/SNF chromatin remodeling complex member *SMARCB1* (also known as hSNF5/INI1) are a characteristic genetic lesion (5, 6). The resulting loss of nuclear SMARCB1 protein expression (7) has been successfully employed to establish the diagnosis of AT/RT also in embryonal tumors lacking rhabdoid features (8, 9) and is nowadays routinely used to distinguish AT/RT from other malignant pediatric brain tumors. The diversity of morphological patterns in AT/RT, however, remained enigmatic, and little is known on associated clinical, genetic, or epigenetic factors.

Recent studies demonstrated three molecular subgroups of AT/RT, namely ATRT-TYR, ATRT-SHH, and ATRT-MYC (10, 11). These molecular subgroups are characterized by distinct DNA methylation signatures, gene expression profiles, and clinical features (12). Because molecular subgrouping has a prognostic role (13) and may predict treatment-specific response and survival in ATRT patients (14), it can be expected

to become a standard of care in the near future. Here we show that the diversity of morphological patterns in AT/RT is related to molecular subgroup status.

2 | MATERIALS AND METHODS

2.1 | Tumor samples

Material from representative paraffin blocks from 114 SMARCB1-deficient AT/RT that had been sent for central review in the context of the European Rhabdoid Registry EU-RHAB was retrieved from the archives of the Institute of Neuropathology Münster (Table 1). EU-RHAB and the tumor bank of the Institute of Neuropathology Münster have received continuous local ethics committee approval (Ethics committee of the University Hospital Münster), and patients or the guardians gave informed consent for the scientific use of archival materials. The diagnosis of AT/RT was confirmed using current WHO criteria and

TABLE 1 Clinical and molecular features

Age [median (interquartile range)]	18 (10–26) months
Sex (male/female)	63/51
<i>Tumor location</i>	
Supratentorial	58 (51%)
Infratentorial	53 (46%)
Spinal	1 (<1%)
Several locations	1 (<1%)
Not available	1 (<1%)
<i>Molecular subgroup</i>	
ATRT-TYR	40 (35%)
ATRT-SHH	48 (42%)
ATRT-MYC	26 (23%)

Note: Clinical and molecular features of 114 AT/RT cases.

routinely included the demonstration of loss of tumoral SMARCB1/INI1 protein expression using immunohistochemistry. DNA methylation profiles have been published previously (13) and were generated using the Methylation EPIC BeadChip array (Illumina, San Diego, CA) and DNA methylation-based classification (15) using the Heidelberg Brain Tumor Classifier (version v11b4) and confirmatory t-distributed stochastic neighbor embedding (TSNE) analyses.

2.2 | Image acquisition and rating

Images of hematoxylin-eosin stained slides were digitally acquired on a Leica SCN400 Slide Scanner up to a 400x magnification and uploaded to an OMERO online platform [version 5.6.2 www.openmicroscopy.org; (16)]. For all slides, tissue area was quantified using the QuPath Software (version 0.2.3) by applying the “simple tissue detection” algorithm at constant parameters.

For evaluation of morphological patterns, slides were independently reviewed by nine observers (four residents and five board-certified neuropathologists). Observers received instructions and a training set of digitalized slides and were then asked to categorize each AT/RT sample in one of four morphological categories: (1) “small-round-blue” comprising AT/RT mainly (>50%) composed of small round blue cells, (2) “mesenchymal” comprising AT/RT with a prevalence (>50%) of spindled cells, desmoplasia and/or myxoid changes, (3) “epithelial,” comprising AT/RT with epithelial features (i.e., formation of surfaces, intratumoral lumina or loosely dehiscent papillary structures) and (4) “rhabdoid” for those AT/RT, in which rhabdoid cells prevailed (>50%; see Figures 1 and 2). Observers were blinded to molecular subgroup status.

2.3 | Immunohistochemistry

Immunohistochemical staining for cytokeratin (MNF-116, Dako M0821, 1:800, proteinase K pretreatment) was performed using the streptavidin-biotin method on an automated staining system (Omnis, DAKO). In a proportion of cases staining results for epithelial membrane antigen, vimentin, actin, GFAP, synaptophysin, and tyrosinase were also available for evaluation.

2.4 | Statistics

Associations between morphological or immunohistochemical categories and molecular subgroup status were examined using chi-square test and the distribution of age and percentages of cytokeratin-positive tumor cells across morphological categories using nonparametric ANOVA. Inter-observer agreement was determined with

Fleiss’ kappa. Specificities and sensitivities were determined for each individual observer and are given as means (range) for the nine observers. Statistical analyses were performed using SPSS (Version 27) and the *irr* and *boot* packages in R (Version 3.6.3). A *p* value <0.05 was considered significant.

3 | RESULTS

The median tissue area represented on the slides accounted for 1.58 cm² (interquartile range: 0.75–2.69 cm²), suggesting that the size of the tissue samples was sufficient for morphological evaluation. The nine observers categorized 34% [26%–46%; mean(range)] of the AT/RT samples as “small-round-blue,” 19% (13–29%) as “epithelial,” 25% (12–44%) as “mesenchymal” and 21% (12%–32%) as “rhabdoid” (Figures 1 and 2). Inter-observer agreement was moderate but highly significant [Fleiss’ kappa = 0.47 (95% confidence interval: 0.41–0.53); *p* < 0.001] and no systematic differences between four novice and five experienced reviewers were observed (Figure 3A,C,E). There was no difference in tumor location between cases rated by the majority of observers as “rhabdoid,” “small-round-blue,” or “mesenchymal,” but a predilection of “epithelial” cases for infratentorial location was noted (chi-square 7.425, df1, *p* = 0.006). Median age was 20.5 months for “rhabdoid,” 18 months for “small-round-blue,” 21 months for “mesenchymal” and only 11.5 months for “epithelial” cases, but this difference did not reach significance.

The series comprised 48 ATRT-SHH, 40 ATRT-TYR, and 26 ATRT-MYC (for details see Table S1). There was a highly significant overall association between morphological categories and molecular subgroup status for all nine observers (*p* < 0.0001; Table S2). Specifically, the category “small-round-blue” was over-represented in ATRT-SHH (Figure 3A, *p* < 0.01) and the category “epithelial” was over-represented in ATRT-TYR (Figure 3C, *p* < 0.000001). The majority of ATRT-MYC were categorized as “mesenchymal” or “rhabdoid,” but this association was less convincing, since only 5/9 observers assigned the category “mesenchymal” significantly more frequently to ATRT-MYC (Figure 3E).

The diagnostic specificity of the morphological category “epithelial” for ATRT-TYR accounted for 97% (mean, range: 88%–99%, Figure 3B), whereas specificities of the categories “small-round-blue” for ATRT-SHH and “mesenchymal” for ATRT-MYC accounted for 83% and 81%, respectively (Figure 3D,F). The sensitivities of “epithelial” for ATRT-TYR, “small-round-blue” for ATRT-SHH and “mesenchymal” for ATRT-MYC were relatively low and accounted for 49%, 57%, and 46%, respectively.

In order to further validate the association of epithelial features and ATRT-TYR, immunohistochemistry for cytokeratin (MNF116) was performed in 107

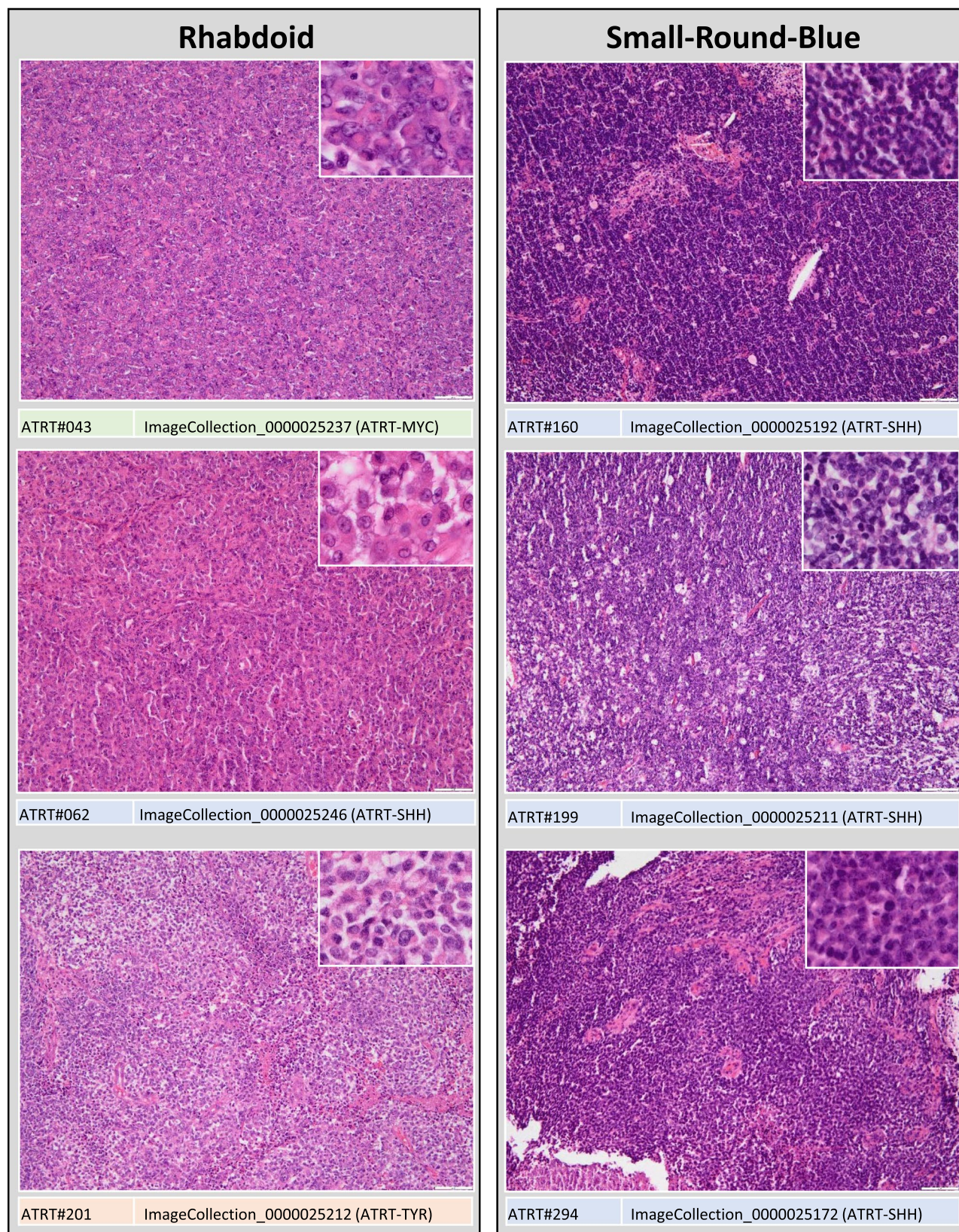


FIGURE 1 Morphological patterns in AT/RT. Shown are three representative examples of each of the morphological categories “rhabdoid” and “small-round-blue.” Scale bars denote 100 μ m.

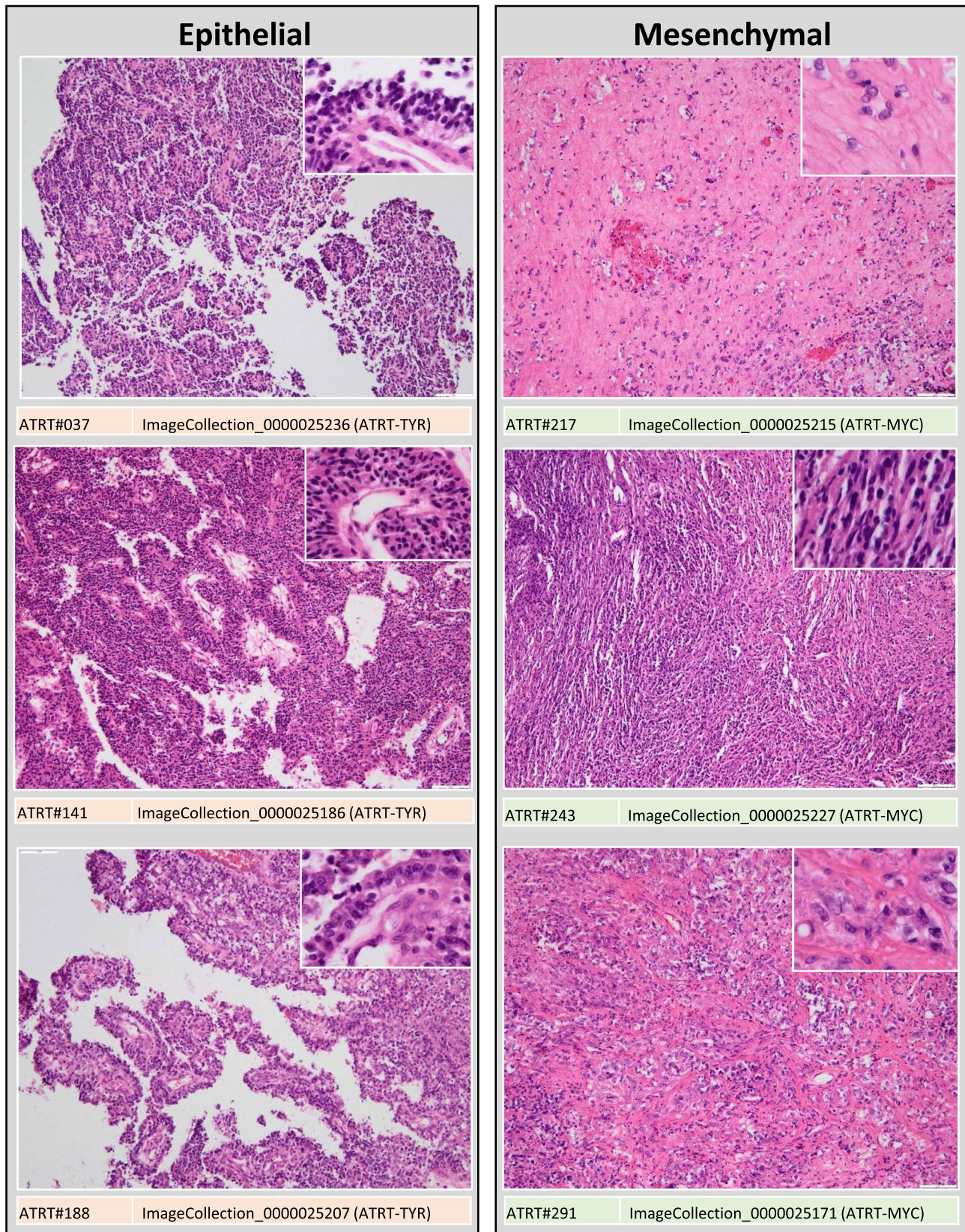


FIGURE 2 Morphological patterns in AT/RT. Shown are three representative examples of each of the morphological categories “epithelial” and “mesenchymal.” Scale bars denote 100 μ m.

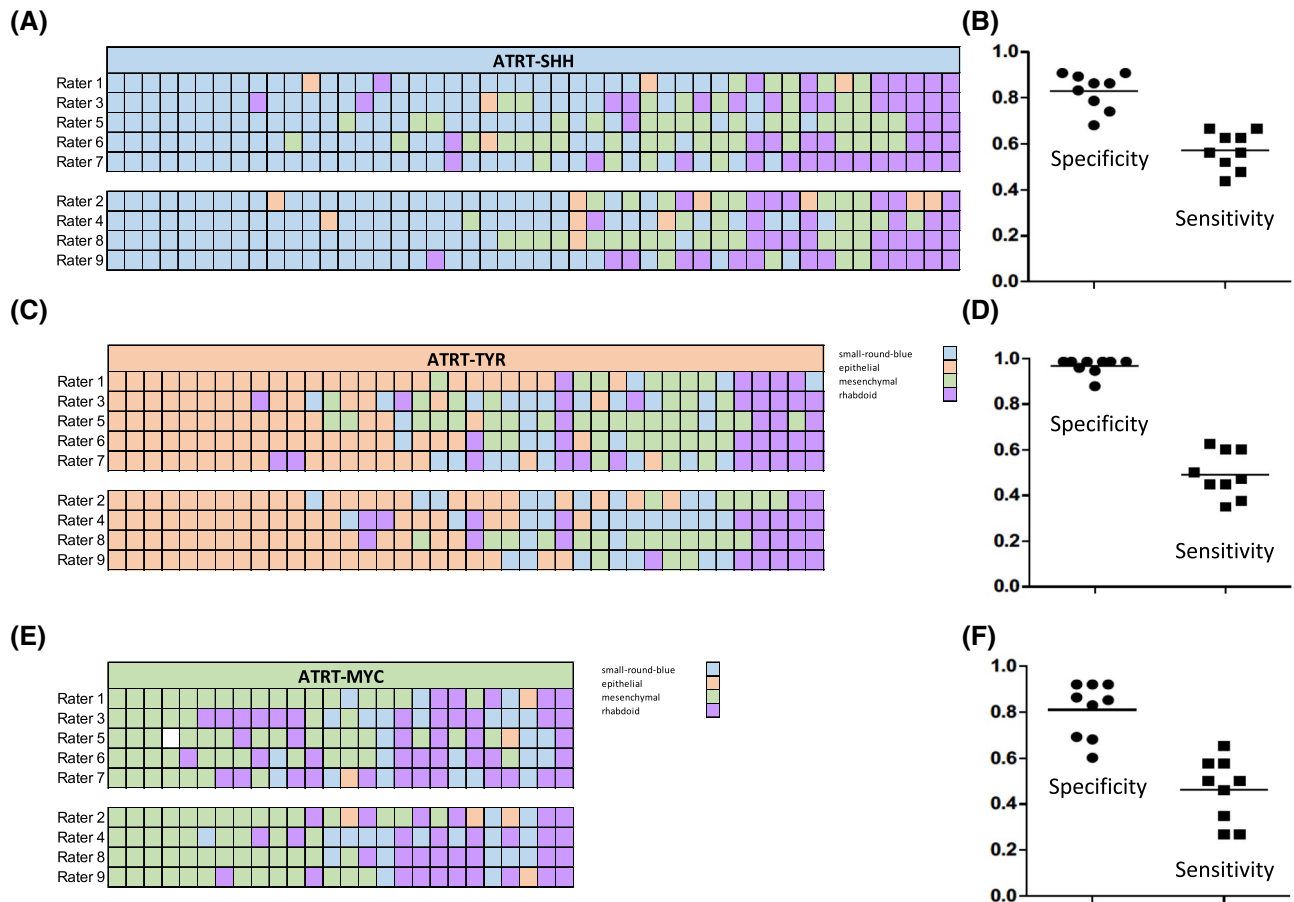


FIGURE 3 Morphological patterns in AT/RT according to molecular subgroup. Distribution of the four morphological categories as rated independently by nine observers according to molecular subgroups ATRT-SHH (A), ATRT-TYR (C), and ATRT-MYC (E). Ratings are color-coded as orange = “epithelial”; blue = “small-round-blue”; green = “mesenchymal”; purple = “rhabdoid”; white = missing data. Note there is no systematic difference between expert (raters 1, 3, 5, 6, 7) and novice (raters 2, 4, 8, 9) observers. Also displayed are the specificities and sensitivities of “small-round-blue” for ATRT-SHH (B) “epithelial” for ATRT-TYR (D), and “mesenchymal” for ATRT-MYC (F)

cases, for which material was available. In line with previous observations (3), a substantial proportion of AT/RT [61/107 (57%)] showed positivity for cytokeratin, often highlighting surfaces but also rhabdoid tumor cells (Figure S1A–C). The proportion of cytokeratin-positive cases was significantly higher in ATRT-TYR as compared to ATRT-SHH and ATRT-MYC (Chi-Square = 35.801, $df = 2$, $p = 0.00000008$). The median percentage of cytokeratin-positive tumor cells was also significantly higher in ATRT-TYR (30.5%) as compared to ATRT-SHH (0%) and ATRT-MYC (3%; Figure S1D). Additional immunohistochemical staining results were available for a proportion of cases (for details see Table S1). All tumors examined stained positive for epithelial membrane antigen (54/54) and vimentin (10/10) and there was no significant difference among molecular subgroups in the proportion of cases positive for actin [ATRT-TYR: 63%, ATRT-SHH: 63%, ATRT-MYC: 75% (Chi-Square: 0.22 $df:2$ $p = 0.89$)], GFAP [ATRT-TYR: 62%, ATRT-SHH: 41%, ATRT-MYC: 33% (Chi-Square: 1.783 $df:2$ $p = 0.41$)] and synaptophysin [ATRT-TYR: 70%, ATRT-SHH: 50%,

ATRT-MYC: 33% (Chi-Square: 1.596 $df:2$ $p = 0.45$)]. In line with our previous observations (12, 17), tyrosinase expression was highly over-represented in the ATRT-TYR molecular subgroup [ATRT-TYR: 83%, ATRT-SHH: 4%, ATRT-MYC: 0% (Chi-Square: 74.022 $df:2$ $p = 1.0E-10$)].

4 | DISCUSSION

The finding that morphological patterns in AT/RT are related to molecular subgroup status suggests that histopathological features might reflect underlying molecular alterations.

The frequency of AT/RT categorized as “small-round-blue,” “mesenchymal,” “epithelial,” and “rhabdoid” resembles the first large series of 52 AT/RT reported by Rorke-Adams (3). In that series, cases showing small round-blue-cell areas were also most frequent (67%), a mesenchymal component was present in 31% of tumors, epithelial features were encountered in 25% of tumors, and 13% solely consisted of rhabdoid tumor cells (3).

Our findings are also well in line with other previous histopathological studies, in which small-round-blue-cell areas were most frequently encountered (18, 19). The authors of one recent series also noted differences of histopathological patterns according to clinical features with tumors showing small-round-blue-cell areas being more frequent in younger children (20). Even though molecular subgroup status was not examined in that study, this finding might well point towards differences of histopathological patterns among molecular subgroups, since patients harboring ATRT-MYC are significantly older (12) and in the present series also rarely were categorized as “small-round-blue.” The subunits of the BAF and PBAF SWI/SNF complexes are central regulators of lineage specification during development. Alterations in these subunits have recently been shown to correlate with the neuronal or epithelial and mesenchymal differentiation in AT/RT (21).

Cases categorized as small-round-blue-cell were overrepresented in ATRT-SHH. The molecular subgroup ATRT-SHH is characterized by a neural expression signature with pathway activation of sonic hedgehog (SHH) and Notch (12). Other small-round-blue-cell tumor entities also display neural expression profiles, suggesting that the predominance of a small-round-blue-cell phenotype in ATRT-SHH might well represent a reflection of its neural expression signature.

Samples categorized as epithelial were overrepresented in ATRT-TYR. ATRT-TYR is characterized by overexpression of tyrosinase (12, 17), which is an important protagonist in neural tube development (22). Our finding that positivity for epithelial marker cytokeratin was also overrepresented in ATRT-TYR, further suggests a link between ATRT-TYR and epithelial differentiation. We have recently shown that cribriform neuroepithelial tumor (CRINET), a rare non-rhabdoid SMARCB1-deficient brain tumor with neuroepithelial histopathology and relatively favorable prognosis (23) shows epigenetic similarities with ATRT-TYR (24). The finding that epithelial features were also overrepresented in ATRT-TYR further suggests similarities of ATRT-TYR and CRINET. As further data become available for these rare tumors it will be interesting to learn whether they represent a unique developmental endpoint of ATRT-TYR.

Finally, ATRT-MYC were often categorized as mesenchymal or rhabdoid, possibly reflecting the epigenetic similarities of this molecular subgroup with extracranial malignant rhabdoid tumors (25), which in addition to a rhabdoid phenotype may also display areas rich in connective tissue and spindled tumor cells (26).

These findings could also be of diagnostic value. Especially the specificity of epithelial features for ATRT-TYR was high. If present, epithelial features might thus give a first hint on the possibility of ATRT-TYR, which will need to be further confirmed by subsequent DNA methylation profiling (12). The same holds true for the

diagnostic value of small-round-blue-cell areas for ATRT-SHH and (to a lesser extent) mesenchymal areas for ATRT-MYC.

One strength of the study is the relatively large number of independent observers. These included experts and trainees from various institutions, suggesting that the results are realistic and could also be applicable in a routine diagnostic setting. We aimed at keeping the rating system simple and chose only a few morphological categories in order to increase the reproducibility of our findings. Even though tissue sections available for morphological examination were relatively large, sampling bias due to tumor heterogeneity cannot be entirely excluded. The fact that the majority of AT/RT contains divergent and transitional histopathological patterns certainly is also contributing to only moderate interobserver agreement. Unsupervised machine learning (27) could be a promising approach to this problem and might aid to identify morphological features associated with molecular subgroups more reproducibly. However, the number of samples for a training cohort would ideally exceed 100 cases per molecular subgroup, a number difficult to achieve especially for ATRT-MYC, which represents only 23% of these rare tumors.

In conclusion, the diversity of morphological patterns in AT/RT is related to molecular subgroup status. Our findings suggest that histopathological features of AT/RT might reflect molecular alterations and may also provide a first hint on molecular subgroup status, which will need to be further confirmed by subsequent DNA methylation profiling.

ACKNOWLEDGMENTS

We thank Dr. Thomas Zobel and the Imaging Network of the Cells in Motion Interfaculty Centre, Westfälische Wilhelms-Universität Münster) for kind support and hosting the OMERO image server, Klavs Grantins (Gerhard-Domagk-Institute of Pathology, University Hospital Münster) for digital slide acquisition and Dr. Raphael Koch (Institute of Biostatistics and Clinical Research, University Hospital Münster) for statistical assistance. This study was supported by DFG (HA 3060/8-1) and IZKF Münster (Ha3/017/20). U.S. is supported by DFG, Wilhelm Sander Stiftung and Fördergemeinschaft Kinderkrebszentrum Hamburg.

CONFLICT OF INTEREST

The authors have no competing interests to declare.

AUTHOR CONTRIBUTIONS

Martin Hasselblatt designed the study together with Francesca Zin. Francesca Zin, Jennifer A. Cotter, Christine Haberler, Matthias Dottermusch, Julia Neumann, Ulrich Schüller, Leonille Schweizer, Christian Thomas, Karolina Nemes, Pascal D. Johann, Marcel Kool, Michael C. Frühwald, Werner Paulus, Alexander Judkins, and Martin Hasselblatt were involved in the

acquisition, analysis, or interpretation of the data. Francesca Zin drafted the manuscript and all co-authors revised it critically for intellectual content.

DATA AVAILABILITY STATEMENT

The data that support the findings of this study are provided in the Supporting Information or are available from the corresponding author upon reasonable request.

ORCID

Ulrich Schüller  <https://orcid.org/0000-0002-8731-1121>
 Martin Hasselblatt  <https://orcid.org/0000-0003-2707-8484>

REFERENCES

- Frühwald MC, Biegel JA, Bourdeaut F, Roberts CW, Chi SN. Atypical teratoid/rhabdoid tumors-current concepts, advances in biology, and potential future therapies. *Neuro Oncol.* 2016;18:764–78.
- Rorke LB, Packer R, Biegel J. Central nervous system atypical teratoid/rhabdoid tumors of infancy and childhood. *J Neurooncol.* 1995;24:21–8.
- Rorke LB, Packer RJ, Biegel JA. Central nervous system atypical teratoid/rhabdoid tumors of infancy and childhood: definition of an entity. *J Neurosurg.* 1996;85:56–65.
- Parham DM, Weeks DA, Beckwith JB. The clinicopathologic spectrum of putative extrarenal rhabdoid tumors. An analysis of 42 cases studied with immunohistochemistry or electron microscopy. *Am J Surg Pathol.* 1994;18:1010–29.
- Biegel JA, Zhou JY, Rorke LB, Stenstrom C, Wainwright LM, Fogelgren B. Germ-line and acquired mutations of INI1 in atypical teratoid and rhabdoid tumors. *Cancer Res.* 1999;59:74–9.
- Jackson EM, Sievert AJ, Gai X, Hakonarson H, Judkins AR, Tooke L, et al. Genomic analysis using high-density single nucleotide polymorphism-based oligonucleotide arrays and multiplex ligation-dependent probe amplification provides a comprehensive analysis of INI1/SMARCB1 in malignant rhabdoid tumors. *Clin Cancer Res.* 2009;15:1923–30.
- Judkins AR, Mauger J, Ht A, Rorke LB, Biegel JA. Immunohistochemical analysis of hSNF5/INI1 in pediatric CNS neoplasms. *Am J Surg Pathol.* 2004;28:644–50.
- Haberler C, Laggner U, Slave I, Czech T, Ambros IM, Ambros PF, et al. Immunohistochemical analysis of INI1 protein in malignant pediatric CNS tumors: Lack of INI1 in atypical teratoid/rhabdoid tumors and in a fraction of primitive neuroectodermal tumors without rhabdoid phenotype. *Am J Surg Pathol.* 2006;30:1462–8.
- Judkins AR, Burger PC, Hamilton RL, Kleinschmidt-DeMasters B, Perry A, Pomeroy SL, et al. INI1 protein expression distinguishes atypical teratoid/rhabdoid tumor from choroid plexus carcinoma. *J Neuropathol Exp Neurol.* 2005;64:391–7.
- Johann PD, Erkek S, Zapatka M, Kerl K, Buchhalter I, Hovestadt V, et al. Atypical teratoid/rhabdoid tumors are comprised of three epigenetic subgroups with distinct enhancer landscapes. *Cancer Cell.* 2016;29:379–93.
- Torchia J, Golbourn B, Feng S, Ho KC, Sin-Chan P, Vasiljevic A, et al. Integrated (epi)-genomic analyses identify subgroup-specific therapeutic targets in CNS rhabdoid tumors. *Cancer Cell.* 2016;30:891–908.
- Ho B, Johann PD, Grabovska Y, De Dieu Andrianteranagna MJ, Yao F, Frühwald M, et al. Molecular subgrouping of atypical teratoid/rhabdoid tumors-a reinvestigation and current consensus. *Neuro Oncol.* 2020;22:613–24.
- Frühwald MC, Hasselblatt M, Nemes K, Bens S, Steinbugl M, Johann PD, et al. Age and DNA methylation subgroup as potential independent risk factors for treatment stratification in children with atypical teratoid/rhabdoid tumors. *Neuro Oncol.* 2020;22:1006–17.
- Hoffman LM, Richardson EA, Ho B, Margol A, Reddy A, Lafay-Cousin L, et al. Advancing biology-based therapeutic approaches for atypical teratoid rhabdoid tumors. *Neuro Oncol.* 2020;22:944–54.
- Capper D, Jones DTW, Sill M, Hovestadt V, Schrimpf D, Sturm D, et al. DNA methylation-based classification of central nervous system tumours. *Nature.* 2018;555:469–74.
- Allan C, Burel JM, Moore J, Blackburn C, Linkert M, Loynton S, et al. OMERO: flexible, model-driven data management for experimental biology. *Nat Methods.* 2012;9:245–53.
- Hasselblatt M, Thomas C, Nemes K, Monoranu CM, Riemenschneider MJ, Koch A, et al. Tyrosinase immunohistochemistry can be employed for the diagnosis of atypical teratoid/rhabdoid tumours of the tyrosinase subgroup (ATRT-TYR). *Neuropathol Appl Neurobiol.* 2020;46:186–9.
- Al-Hussaini M, Dissi N, Souki C, Amayiri N. Atypical teratoid/rhabdoid tumor, an immunohistochemical study of potential diagnostic and prognostic markers. *Neuropathology.* 2016;36:17–26.
- Sali AP, Epari S, Nagaraj TS, Sahay A, Chinnaswamy G, Shetty P, et al. Atypical teratoid/rhabdoid tumor: revisiting histomorphology and immunohistochemistry with analysis of cyclin D1 overexpression and MYC amplification. *Int J Surg Pathol.* 2021;29(2):155–164.
- Wang RF, Guan WB, Yan Y, Jiang B, Ma J, Jiang MW, et al. Atypical teratoid/rhabdoid tumours: clinicopathological characteristics, prognostic factors and outcomes of 22 children from 2010 to 2015 in China. *Pathology.* 2016;48:555–63.
- Panwalkar P, Pratt D, Chung C, Dang D, Le P, Martinez D, et al. SWI/SNF complex heterogeneity is related to polyphenotypic differentiation, prognosis, and immune response in rhabdoid tumors. *Neuro Oncol.* 2020;22:785–96.
- Simoes-Costa M, Bronner ME. Establishing neural crest identity: a gene regulatory recipe. *Development.* 2015;142:242–57.
- Hasselblatt M, Oyen F, Gesk S, Kordes U, Wrede B, Bergmann M, et al. Cribriform neuroepithelial tumor (CRINET): a non-rhabdoid ventricular tumor with INI1 loss and relatively favorable prognosis. *J Neuropathol Exp Neurol.* 2009;68:1249–55.
- Johann PD, Hovestadt V, Thomas C, Jeibmann A, Hess K, Bens S, et al. Cribriform neuroepithelial tumor: molecular characterization of a SMARCB1-deficient non-rhabdoid tumor with favorable long-term outcome. *Brain Pathol.* 2017;27:411–8.
- Chun HE, Johann PD, Milne K, Zapatka M, Buellesbach A, Ishaque N, et al. Identification and analyses of extra-cranial and cranial rhabdoid tumor molecular subgroups reveal tumors with cytotoxic T cell infiltration. *Cell Rep.* 2019;29:2338–54.e7.
- Weeks DA, Beckwith JB, Mierau GW. Rhabdoid tumor. An entity or a phenotype? *Arch Pathol Lab Med.* 1989;113:113–4.
- Roohi A, Faust K, Djuric U, Diamandis P. Unsupervised machine learning in pathology: the next frontier. *Surg Pathol Clin.* 2020;13:349–58.

SUPPORTING INFORMATION

Additional Supporting Information may be found online in the Supporting Information section.

FIGURE S1 Cytokeratin immunohistochemistry. Staining patterns for cytokeratin (MNFI16) in AT/RT. Note highlighted epithelial surfaces in two representative ATRT-TYR cases (A and B), while only scattered rhabdoid tumor cells stain positive in a case of ATRT-MYC (C). On quantification of positive tumor cells in 107 AT/RT samples (D), significantly higher median percentages

are encountered in ATRT-TYR as compared to MYC ($p = 0.18$) and SHH ($p < 0.0001$; non-parametric ANOVA followed by Mann-Whitney-*U*-Test)

TABLE S1 Clinical and molecular features, available immunohistochemical staining results as well as the rating of morphological patterns by nine individual observers (initials)

TABLE S2 Detailed chi-square statistics

How to cite this article: Zin F, Cotter JA, Haberler C, et al. Histopathological patterns in atypical teratoid/rhabdoid tumors are related to molecular subgroup. *Brain Pathology*. 2021;31:e12967. <https://doi.org/10.1111/bpa.12967>